

# A Novel Compact Ultra-Wideband Planar Inverted-L Antenna For Wireless Application

Iman Ben Issa, and Mohamed Essaaidi

**Abstract**—A novel compact Ultra-Wide-Band Planar Inverted-L antenna is presented and investigated in this paper. The proposed antenna consists of a square planar radiating element with a U-shaped slot. The radiating element is supported by a shorting wall, and fed by a single 50 Ohms characteristic impedance microstrip line, printed on the top of the FR-4 substrate. The ground plane of the antenna is printed on the other side of the substrate. The entire antenna occupies only a small volume of  $20\text{mm} \times 35\text{mm} \times 4\text{mm}$ , and is capable of operating from 4.2GHz to 8.6GHz (68.75%) and offers a maximum gain of 5.24dB. Therefore, it is suitable for UWB systems and other wireless and mobile technologies and, thus, can be integrated into smartwatch, mobile phones, tablets and laptops. The design of this antenna was carried out using 3D software such as CST studio and Ansoft HFSS to compare and validate the results.

**Keywords**—compact; planar inverted-L antenna; ultra-wideband; wireless application

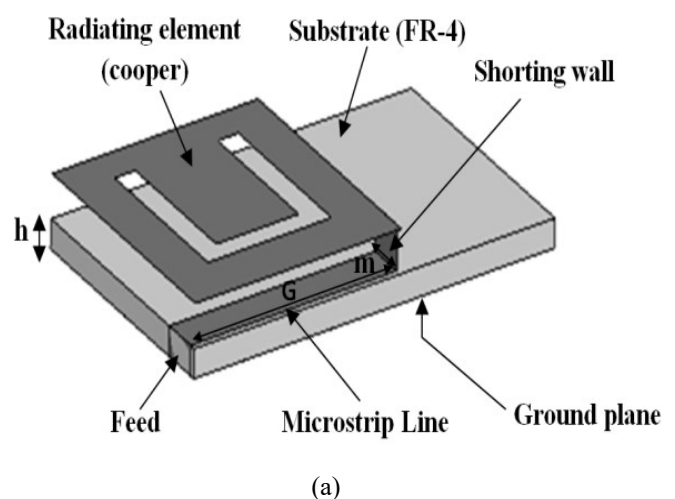
## I. INTRODUCTION

IN modern mobile and wireless communications systems, there is an increasing demand for compact antenna that can be easily integrated into the portable devices such as smart phones, organizers, tablets, computers, navigation devices, etc... In this regard, microstrip patch antennas are an attractive alternative in modern mobile and wireless communications systems, because of their characteristics such as ease of fabrication, integration compactness, low profile and lightweight. Nevertheless, the dimensions of the patch for an antenna operating in its fundamental mode may be too large for some practical applications. Several techniques have been proposed and reported in the literature to achieve patch size miniaturisation. The most well known techniques consist of using high-dielectric-constant material [1, 2] loading the patch with an inductive notch or slot [3, 4], irregular ground plane [5] and using a folded patch [6, 7], such as PIFA (Planar Inverted F Antenna) and PILA (Planar Inverted L Antenna). This last is rarely used, this is because it suffers a narrow impedance bandwidth in their basic form, that has only a single feed and no grounding pin. This drawback has restricted their broadband applications. Several techniques have been developed to alleviate the narrow impedance bandwidth problem. Modifying the radiating elements is one of the main methods, using MIMO technology [8, 9] or modifying the feed by adding a dielectric slab between two strips (fed strip and grounded strip) [10]. In

this paper, a novel ultra-wideband planar inverted-L antenna is presented. Using microstrip line feed connected to a shorting wall, the operating frequency band of this antenna ranges from 4.2 to 8.6 GHz, The total dimension of the antenna structure is  $20\text{mm} \times 35\text{mm} \times 4\text{mm}$ . So, it can be easily integrated with other RF fond-end circuitry in small size portable mobile, Smartwatch and wireless handsets for modern and emerging communications.

## II. ANTENNA CONFIGURATION

The geometry of the proposed UWB-PILA is shown in Fig. 1. The antenna composed of a square planar radiating element of size  $20\text{mm} \times 20\text{mm}$ , with a U-shaped slot located in the center. The radiating element is supported by a shorting wall with a height of  $H=2.4\text{mm}$  and width of  $m=3\text{mm}$ , connected to microstrip-line of 50 Ohms with a dimension of  $3\text{mm} \times 20\text{mm}$ , printed on top of the FR-4 substrate (relative dielectric constant of 4.4 and a thickness of 1.6mm). The ground plane of the antenna is printed on the other side of the substrate. A rectangular notch cut on the ground plane, is introduced exactly behind the transmission line. This leads to better impedance matching over the entire obtained a wide bandwidth. The total dimension of the antenna structure is  $20\text{mm} \times 35\text{mm} \times 4\text{mm}$ . The design parameters of the UWB-PILA are given in Table I.



This work was supported by Faculty of Science-Tetuan, Abdelmalek Essaadi University, Morocco.

Iman BEN ISSA is with Department of Physics, Abdelmalek Essaadi University, Faculty of Science, Tetuan, Morocco (email: [benissa.iman@hotmail.com](mailto:benissa.iman@hotmail.com)).

Mohamed ESSAAIDI is with High National School for Computer Science and Systems Analysis- Rabat, Mohammed V University, Rabat, Morocco; (email: [m.essaaidi@ieee.ma](mailto:m.essaaidi@ieee.ma)).



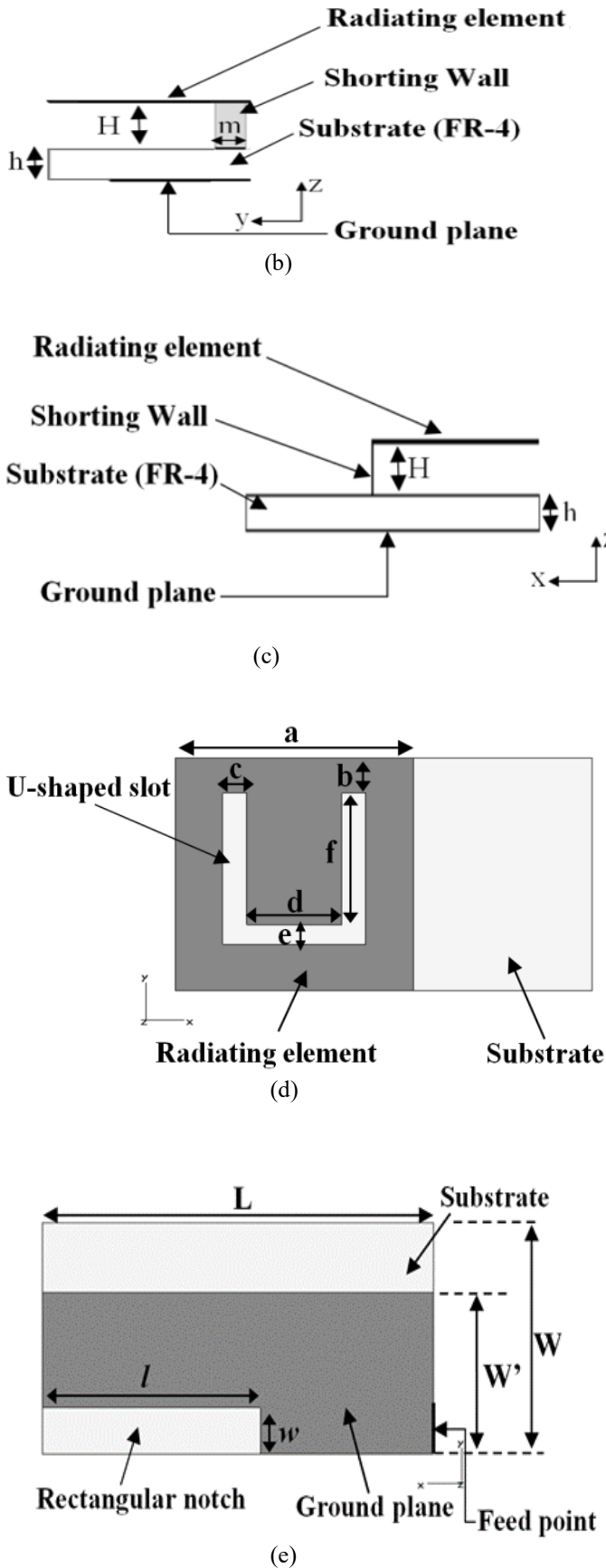


Fig.1. Geometry of the antenna (a) 3D view, (b) front view (c) side view, (d) top view, (e) bottom view.

TABLE I  
DIMENSIONS OF THE PROPOSED ANTENNA

Parameters	Values (mm)
Sides of the square radiating element : a	20
U-slot parameters: b, c, d, e, f	3, 2, 8, 1.7, 11.3
Height of shorting wall : H	2.4
Width of shorting wall and microstrip line : m	3
Length of microstrip line G	20
Width of ground plane : W'	14
Length of the rectangular notch of the ground plane : l	19.5
Width of the rectangular notch of the ground plane : w	4
Length of Substrate : L	35
Width of substrate : W	20
The thickness of substrate : h	1.6
Substrate	FR-4( $\epsilon_r = 4.4$ )

### III. EFFECTS OF KEY PARAMETERS

In order to get adequate information of the antenna operation mechanics, the effects of geometric parameters on antenna bandwidth are investigated. The parameters  $W'$ ,  $l$ ,  $d$ ,  $f$  and  $m$  are selected in the parametric study. To accurately understand the influence of these parameters on its impedance bandwidth, only one parameter is studied at each time while others are kept constant. Some important observations have been made during the design concerning the variation of several parameters. These parameters contribute largely in achieving the ultra-wide-band behavior. The effect of each parameter is shown in Fig. 2, Fig. 3, Fig. 4, Fig. 5 and Fig. 6.

Fig. 2 shows the return loss of the antenna with different values of  $W'$ , and the values of  $l$ ,  $d$ ,  $f$  and  $m$  are fixed at 19.5mm, 8mm, 11.3mm and 3mm, respectively. It is clearly seen that this parameter affects the whole frequency range. when  $W'$  is between 16 mm and 20 mm (i.e.  $16\text{mm} \leq W' \leq 20\text{mm}$ ), the antenna has a multiband frequency response. When  $W' = 12$  mm or 14 mm, the matching is improved in all the frequency band, and ultra-wide-band behavior is achieved. The optimal value which corresponds to the best impedance matching is  $W' = 14$ mm. Fig. 3 shows the return loss of the antenna with different values of  $l$ , while  $W'$ ,  $d$ ,  $f$  and  $m$  are maintained at a fixed value of 14mm, 8mm, 11.3mm and 3mm, respectively. It can be noted that the variation of  $l$  from 0 to 15mm makes the bandwidth of the antenna narrower. For other values of  $l$  higher than 15 mm, the antenna shows a dual-band behavior. The matching of the antenna is better when  $l = 19.5$ mm. The insertion of a slot in the ground plane increases significantly the bandwidth from 3.35% to 68.75%.

To study the influence of the U-shaped slot of the radiating element on the antenna bandwidth, we vary the parameter  $d$  values while those of  $W'$ ,  $l$ ,  $f$  and  $m$  are maintained at 14mm, 19.5mm, 11.3mm and 3mm, respectively. Then we varied the value of the parameter  $f$ , while those corresponding to  $W'$ ,  $l$ ,  $d$  and  $m$  are maintained fixed at 14 mm, 19.5 mm, 8 mm and 3 mm, respectively. As shown in Fig. 4, the parameter  $d$  affects primarily the range of frequencies between 4.2GHz and 7.2GHz.

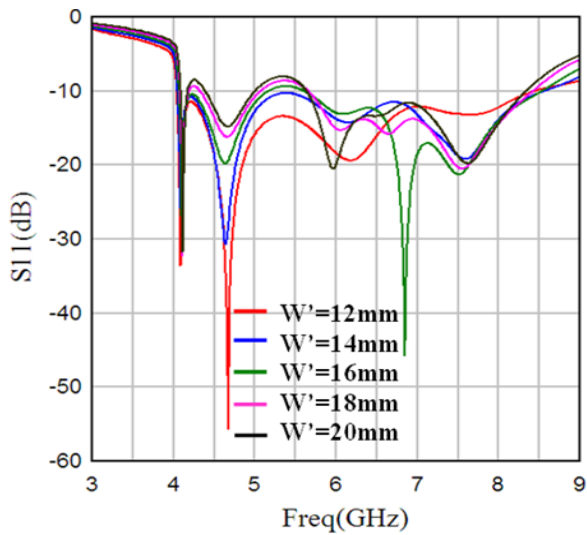


Fig. 2. Return loss versus frequency for different  $W'$  values ( $l = 19.5$  mm,  $d = 8$  mm,  $f = 11.3$  mm and  $m = 3$  mm)

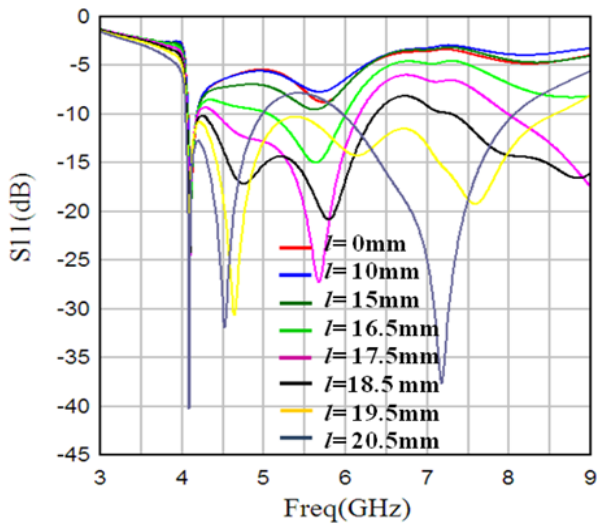


Fig. 3. Return loss versus frequency for different  $l$  values ( $W' = 14$  mm,  $d = 8$  mm,  $f = 11.3$  mm and  $m = 3$  mm)

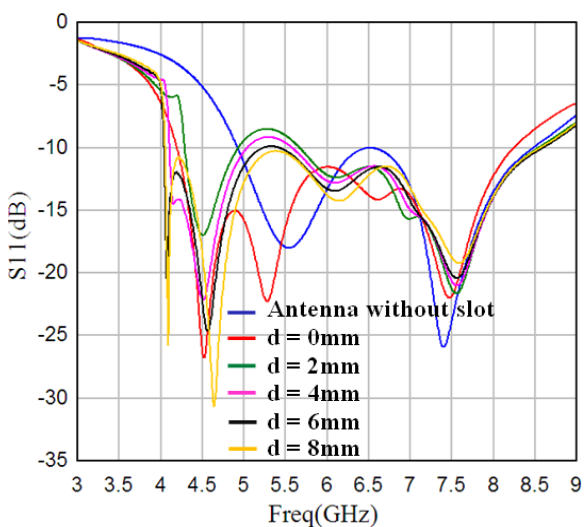


Fig. 4. Return loss versus frequency for different  $d$  values ( $W' = 14$  mm,  $l = 19.5$  mm,  $f = 11.3$  mm and  $m = 3$  mm).

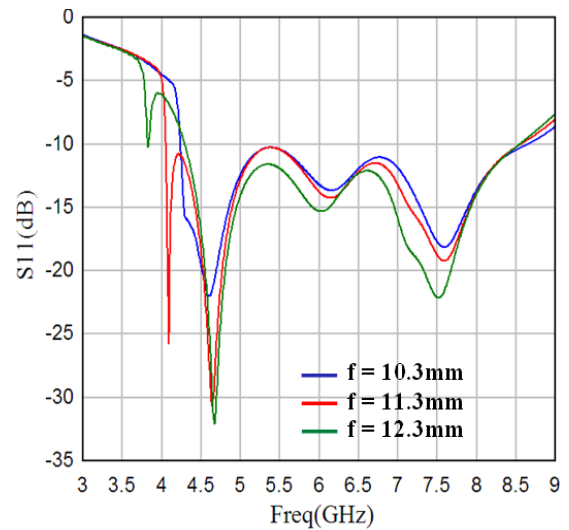


Fig. 5. Return loss versus frequency for different  $f$  values ( $W' = 14$  mm,  $l = 19.5$  mm,  $d = 8$  mm and  $m = 3$  mm).

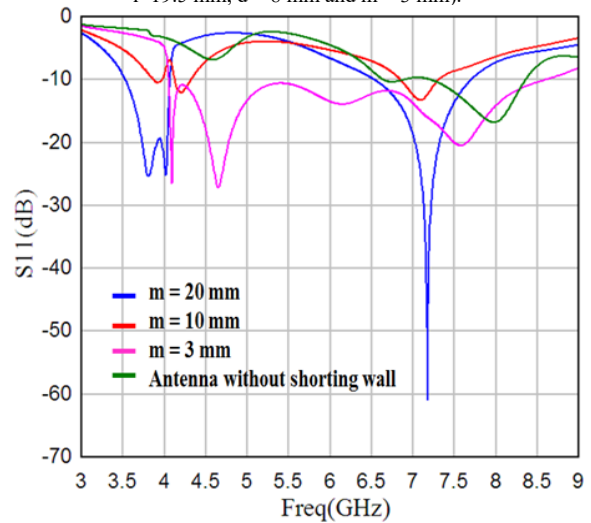


Fig. 6. Return loss versus frequency for different  $m$  values ( $W' = 14$  mm,  $l = 19.5$  mm,  $d = 8$  mm and  $f = 11.3$  mm).

We note that the antenna has an optimal ultra-broadband operation and corresponds to a good adaptation when  $d = 8$  mm. Fig. 5 shows an optimal ultra-broadband operation for the value  $f = 11.3$  mm. By comparing the reflection coefficient of the antenna with and without the U-shaped slot, it is observed that, the width of the bandwidth of the 'UWB-PILA' without the slot is 53.73% (4.9 GHz to 8.5 GHz). However, in the presence of the slot, the bandwidth of the antenna is increased to 68.75% (4.2 GHz to 8.6 GHz). Therefore, the slot contributes to the widening of the bandwidth and to the miniaturization of the antenna (see Fig. 4). Fig. 6 shows the effect of the shorting wall on the bandwidth response. We vary the parameter  $m$  values while those of  $W'$ ,  $l$ ,  $d$  and  $f$  are maintained fixed at 14 mm, 19.5 mm, 8 mm and 11.3 mm, respectively. It can be noted that in the absence of the shorting wall, the impedance bandwidth is reduced. It is also observed that for  $m = 20$  mm, and  $m = 10$  mm the antenna is able to operate as a multiband antenna. However, the return loss of the antenna improves when the width of the wall  $m$  decreases to  $m = 3$  mm. From these results we can say that the shorting-wall also contributes to the enlargement of the

bandwidth of the antenna, when its width 'm' is equal to the width of the feed-line ( $m = 3$  mm).

#### IV. RESULTS AND DISCUSSION

In this section, we present and discuss the frequency response of the UWB-PILA and its characteristics, namely, the reflection coefficient, the radiation pattern and the gain. These results are obtained through simulations carried out using CST simulator [11]. For the sake of comparison and validation of these results another commercial EM simulator is used which is Ansoft HFSS [12].

##### A. Reflection coefficient

Fig. 7 shows the simulated reflection coefficients of the UWB-PILA antenna. A reasonable agreement is observed between the two results, namely, the plots for  $S_{11} \leq -10$  dB impedance bandwidth. The intersection of these two results, covers a band from 4.2 GHz to 8.6 GHz (68.75%).

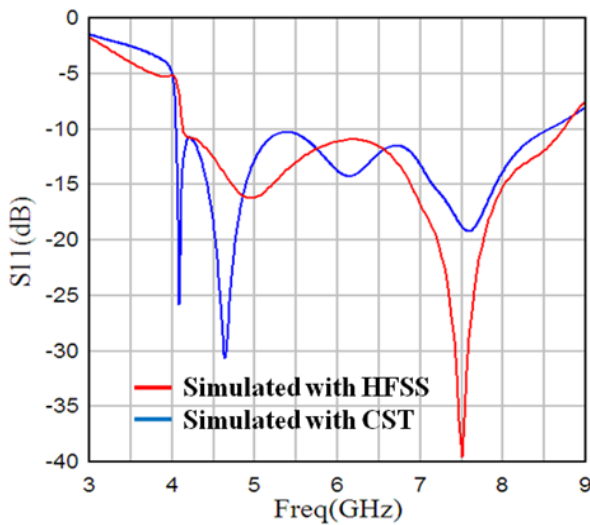
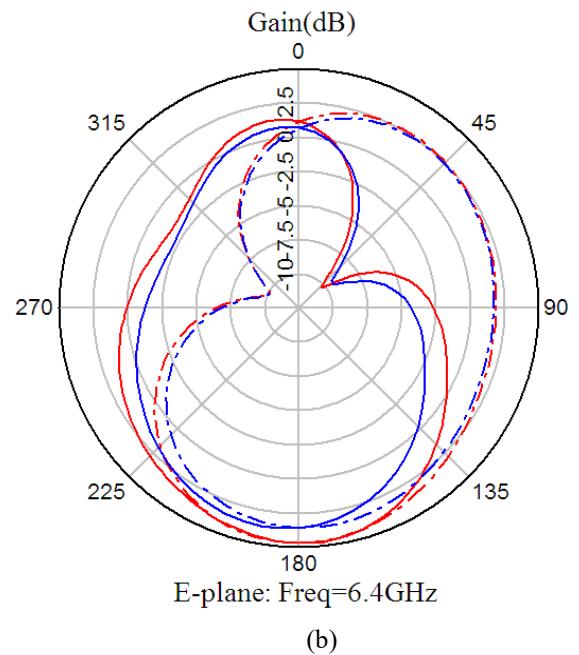
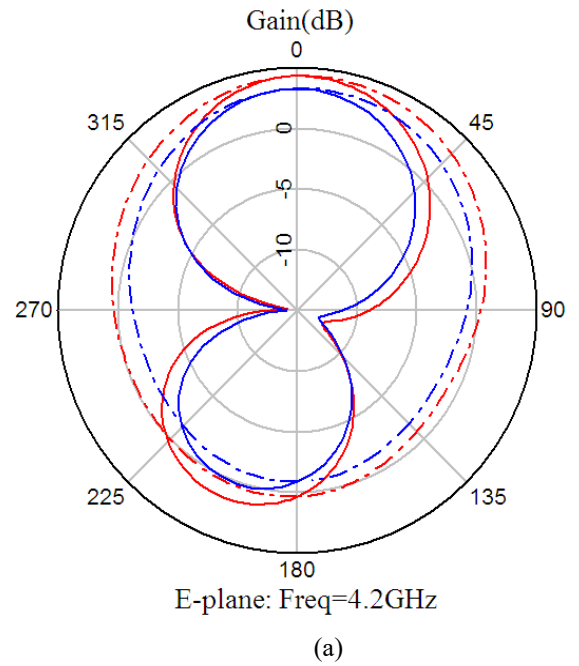


Fig. 7. Reflection coefficients of the proposed UWB antenna

##### B. Radiation Patterns

The radiation patterns of the proposed antenna at 4.2GHz, 6.4GHz and 8.6GHz are illustrated in Fig. 8. These radiation patterns are presented for two elevation planes: XZ ( $\phi = 0^\circ$ ) and YZ ( $\phi = 90^\circ$ ). It is observed that for the frequency of 4.2GHz, in the E-plane  $\phi = 0^\circ$ , the radiation pattern is bidirectional. However, in the E-plane  $\phi = 90^\circ$ , the radiation pattern is nearly omnidirectional (see Fig. 8a). At the frequency of 6.4 GHz, the radiation pattern is quasi-bidirectional for both E-plane ( $\phi = 0^\circ$  and  $\phi = 90^\circ$ ) (see Fig. 8b). At the frequency of 8.6 GHz, the radiation pattern has a multi-directional behavior for E-plane  $\phi = 0^\circ$ . However, in the E-plane  $\phi = 90^\circ$ , the radiation pattern is quasi-bidirectional (see Fig. 8c).



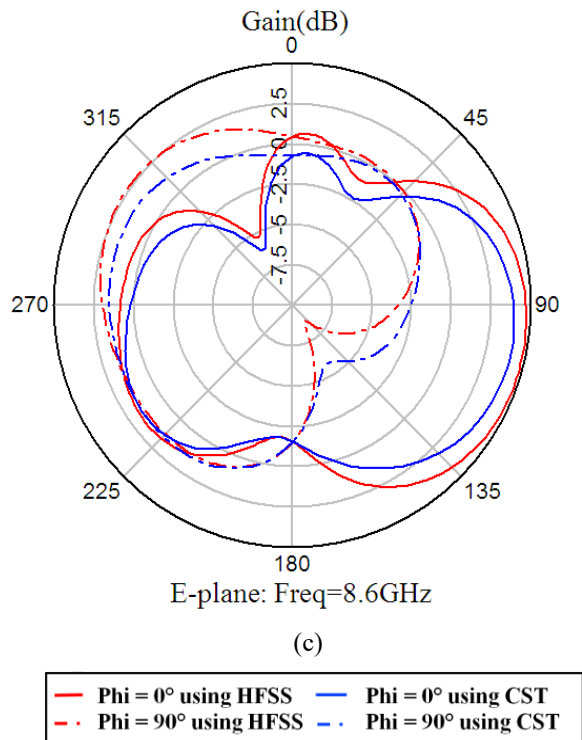


Fig. 8. Simulated radiation patterns of proposed antenna (a) 4.2 GHz, (b) 6.4 GHz and (c) 8.6 GHz

### C. Gain

Fig. 9 shows the gain of the proposed UWB-PILA antenna, simulated by the two simulators Ansoft HFSS and CST. We note that according to the obtained gain values, the maximum gain of this antenna is 5.24dB at a frequency of 7GHz. Thus, this antenna is extremely suitable for operation for UWB wireless technology systems.

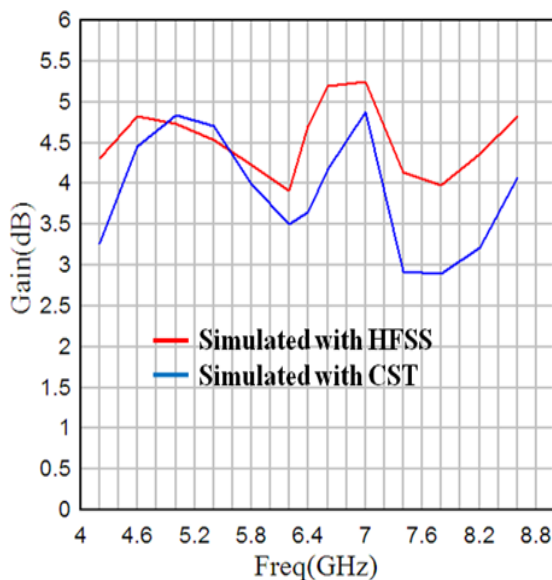


Fig. 9. Gain of the proposed antenna

### CONCLUSION

A novel ultra-wideband planar inverted-L antenna is designed, and characterized in details. The proposed antenna has a compact size of 20mm x 35mm x 4mm. So it can be integrated into smartwatch, mobile phones, tablets and laptops. Computer simulations using both commercial simulators, namely, CST Studio Suite and Ansoft HFSS, that have indicated a good agreement between the obtained results. This antenna can be applied to modern speed wireless communication technologies in the frequency band ranging from 4.2GHz to 8.6GHz (68.75%). It can offers a maximum gain of 5.24dB, what makes it useful for both indoor and outdoor wireless communications.

### REFERENCES

- [1] B. Lee and F. Harackiewicz, "Miniature microstrip antenna with a partially filled high-permittivity substrate," *IEEE Trans. Antennas Propag.*, vol. 50, no. 8, pp. 1160–1162, Aug. 2002. <http://doi.org/10.1109/TAP.2002.801360>
- [2] T. Lo, C.-O.Ho, Y. Hwang, E. K.W. Lam, and B. Lee, "Miniature aperture coupled microstrip antenna of very high permittivity," *Electron. Lett.*, vol. 33, no. 1, pp. 9–10, 1997. <http://doi.org/10.1049/el:19970053>
- [3] S. Reed, L. Desclos, C. Terret, and S. Toutain, "Patch antenna size reduction by means of inductive slots," *Microw. Opt. Technol. Lett.*, vol. 29, no. 2, pp. 79–81, 2001. <https://doi.org/10.1002/mop.1089>
- [4] X. Cheng, J. Wu, R. Blank, D. Senior, and Y.-K. Yoon, "An omnidirectional wrappable compact patch antenna for wireless endoscope applications," *IEEE Antennas Wireless Propag. Lett.*, vol. 11, pp. 1667–1670, 2012. <https://doi.org/10.1109/LAWP.2013.2238600>
- [5] D. Wang, H. Wong, and C. H. Chan, "Small patch antennas incorporated with a substrate integrated irregular ground," *IEEE Trans. Antennas Propag.*, vol. 60, no. 7, pp. 3096–3103, Jul. 2012. <https://doi.org/10.1109/TAP.2012.2196915>
- [6] S. Pinhas and S. Shtrikman, "Comparison between computed and measured bandwidth of quarter-wave microstrip radiators," *IEEE Trans. Antennas Propag.*, vol. 36, no. 11, pp. 1615–1616, Nov. 1988. <https://doi.org/10.1109/8.9713>
- [7] R. Chair, K. F. Lee, and K. M. Luk, "Bandwidth and cross-polarization characteristics of quarter-wave shorted patch antennas," *Microw. Opt. Technol. Lett.*, vol. 22, no. 2, pp. 101–103, 1999. [https://doi.org/10.1002/\(SICI\)1098-2760\(19990720\)22:2<101::AID-MOP7>3.0.CO;2-X](https://doi.org/10.1002/(SICI)1098-2760(19990720)22:2<101::AID-MOP7>3.0.CO;2-X)
- [8] S. Alja'afreh, Y. Huang, Q. Xu, L. Xing and O. A. Saraereh, "MIMO antenna system of a compact 4-element PILA for 4G handset applications," 2016 Loughborough Antennas & Propagation Conference (LAPC), Jan. 2017. <https://doi.org/10.1109/LAPC.2016.7807482>
- [9] S. Alja'afreh, Y. Huang, L. Xing, Q. Xu and X. Zhu, "A Low Profile and Wideband PILA-based Antenna for Handset Diversity Applications," *IEEE Antennas and Wireless Propagation Letters*, vol. 14, pp. 923 – 926, Dec 2014. <https://doi.org/10.1109/LAWP.2014.2384834>
- [10] Z. N. Chen, M. Y. W. Chia, "Broadband planar inverted-L antennas," *IEE Proceedings - Microwaves Antennas and Propagation*, vol. 148, no. 5, pp. 339 – 342, Oct 2001. <https://doi.org/10.1049/ip-map:20010729>
- [11] "Computer Simulation Technology", CST STUDIO SUITE. [Online] [www.cst.com](http://www.cst.com)
- [12] "High Frequency Structure Simulator", Ansoft LLC. [Online] [www.ansys.com](http://www.ansys.com)